Available online at www.sciencedirect.com

ScienceDirect

Journal of Ocean Engineering and Science 1 (2016) 119–128

www.elsevier.com/locate/joes

A comparison between Smoothed-Particle Hydrodynamics and RANS Volume of Fluid method in modelling slamming

Marcus Sasson, Shuhong Chai*, Genevieve Beck, Yuting Jin, Jalal Rafieshahraki

National Centre for Maritime Engineering and Hydrodynamics, Australian Maritime College, University of Tasmania, Launceston, Tasmania, Australia

Received 31 August 2015; received in revised form 30 October 2015; accepted 30 November 2015
Available online 14 March 2016

Abstract

The oil and gas industry requires complex subsea infrastructure in order to develop offshore oil and gas fields. Upon installation, these components may encounter high slamming loads, stemming from impact with the water surface. This paper utilises two different numerical methods, the mesh-free Smoothed Particle Hydrodynamics (SPH) approach and Reynolds Averaged Navier–Stokes (RANS) Volume of Fluid (VOF) method to quantify these loads on a free-falling object. The investigation is also interested in conducting a parameter study and determining the effect of varying simulation parameters on the prediction of slamming event kinematics and forces. The surface impact of a freefalling wedge was introduced as a case study and has been simulated using SPH and RANS, with the results being compared to an experimental investigation. It was found from the SPH simulations that particle resolution and the size of the SPH particle kernel are very important, whilst the diffusion term does not play an important role. The latter is due to the very transient nature of slamming events, which do not allow sufficient time for diffusion in the fluid domain. For the RANS simulations, motion of the wedge was achieved using the overset grid technique, whereby varying the discretising time step was found to have a pronounced impact on the accuracy of the captured slamming event. Through analysing the numerical data, one can observe that the RANS results correlate slightly better with the experimental data as opposed to that obtained from the SPH modelling. However, considering the robustness and quick set up of the SPH simulations, both of these two numerical approaches are considered to be promising tools for modelling more complicated slamming problems, including those potentially involving more intricate structures.

Keywords: Smoothed Particle Hydrodynamics; Reynolds Averaged Navier–Stokes; Slamming load; Wedge.

1. Introduction

The development of offshore oil and gas fields requires a large amount of subsea infrastructure to aid in the production and transport of reservoir fluids. This infrastructure is usually highly expensive and is not built with a significant level of redundancy, meaning that a failure can result in a complex and costly replacement operation. One cause of failure that has not been thoroughly investigated is the slamming load created during installation, which can weaken the structure.

Slamming events are defined by a high load that is exerted on a body over a short period of time [10]. They occur when a body impacts the water surface at relatively low-deadrise angles, resulting in a sudden expansion in the contact area between the fluid body and contact surface [12]. The very fast transient rise of pressures on the surface in slamming situations can cause local structural damage, while absorption of slam loads can cause global structural failure. Slamming loads can also excite modal vibration in the structure, imposing high cyclic loads and reducing the fatigue life of the structure. They may also permanently weaken the structure and increase its chance of failure at loads below the initial design considerations.

Many forms of investigation have been conducted to quantify the loading arising from slamming events. This includes full-scale experiments, laboratory model experiments of rigid or hydroelastic structures, and analytical/numerical solutions. The mathematical models include early works from Wagner [20] using momentum theory and expand to modern day

* Corresponding author.
E-mail address: shuhong.chai@utas.edu.au (S. Chai).

http://dx.doi.org/10.1016/j.joes.2016.03.004

techniques that encompass rigid or hydroelastic structures in a meshed or mesh free fluid domain.

SPH is a mesh free method, first developed by Gingold and Monaghan [6] for astronomical problems and further utilised in free surface flows by Monaghan [16]. Since then, SPH has been progressively refined for use in hydrodynamic and hydraulic problems. Unlike traditional meshed methods, SPH is especially useful for the analysis of high velocity impacts where the fluid boundary experiences high degrees of deformation [14], making it particularly effective in analysing slamming problems. Many fast transient problems such as dam-breaks and sloshing have been modelled successfully by SPH [9]. Recent developments in SPH modelling include the use of Graphic Processing Units (GPU) and of new neighbour search algorithms, which have significantly reduced the computational time of the simulation process [1,4]. Furthermore, Oger et al. [17] modelled free falling two - dimensional (2D) wedges in SPH; obtaining good correlation with experimental results.

Due to the advancement and availability of computational power, a new solution by way of RANS to resolve complex fluid problems is becoming more feasible for industry applications. It utilises discrete methods to apply a system of partial differential equations to flow-driven applications. An example of current literature utilising this approach to model slamming includes a study by Johannessen [11] on the testing of a lifeboat design in free fall during the impact phase. Additionally, a study by Larsen [13] uses similar analytical measures to focus on water entry for circular cylinders. It was concluded from both of these studies that RANS produces good correlation between pre-existing data obtained from experimental or alternative methods [11,13].

In this paper, a benchmark wedge free falling case study has been conducted using open source SPH code, DualSPHysics, (Crespo et al. [1]; Gomez-Gesteira et al. [8]; Gomez-Gesteira et al. [7]) and commercial RANS solver, Star-CCM+ [2]. The results were reviewed to assess the feasibility and accuracy of these two numerical approaches in modelling slamming. For the SPH simulations, the impact of altering smoothing length and artificial viscosity was investigated. A particle resolution study was also completed within a range of relatively small particle sizes. For the RANS simulations, a time step sensitivity study has been conducted to investigate the impact of discretising the time step on the slamming model. The kinematics of both SPH and RANS modelled wedge impacts were then compared with experimental results from Whelan [21] to ensure their accuracy.

1.1. Benchmark experiment description

The wedge free falling experiment conducted by Whelan [21] was analysed to validate his numerical model of catamaran slamming. The physical dimensions of the model are shown in Table 1 and Fig. 1. For model scaling, the normalised drop height, H^* was defined as:

$$H^* = \sqrt{\frac{2H}{L}} \tag{1}$$

Table 1
Freefalling wedge geometry.

Properties	Value
L	0.50 (m)
D	0.07 (m)
α	25 (degrees)

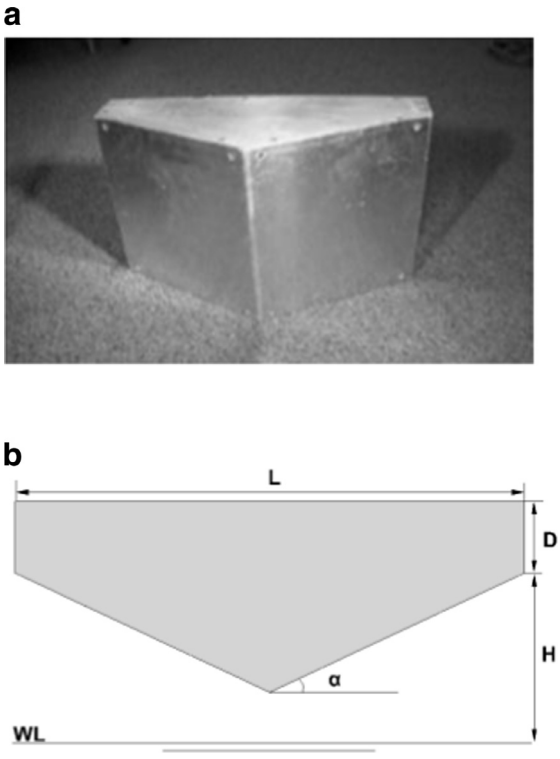

Fig. 1. Wedge geometry from Whelan [21].

where $H$is the drop height from the free surface to side corners and L is the beam of the model. The value of $H^*$was chosen to be 1.08 as it is equivalent to an effective Froude number when considering the water entry process.

2. SPH technique

2.1. SPH theory overview

SPH is a mesh-free method that utilises an array of particles to form the simulation domain. These particles represent an interpolation grid that is used to compute the fluid properties at any given point in the simulation domain by using an interpolation function called the 'Kernel'. This is used to discretise the partial differential equations without the use of a mesh; modelling the fluid behaviour [17]. A visual representation of this system is displayed below in Fig. 2.

SPH utilises Eq. (2) to interpolate the properties of any given particle using its neighbouring particles within the influence domain [15].

$$A(\vec{r}) = \int_V A(\vec{r}')W(\vec{r} - \vec{r}', h)d\vec{r}' \tag{2}$$

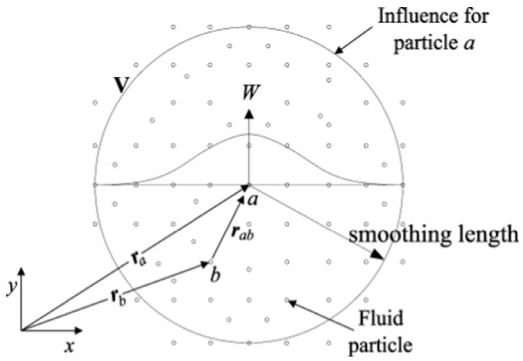

Fig. 2. Particle interactions in SPH within the influence domain governed by the kernel function [19].

where

$A(\vec{r})$ = Any given characteristic
$W(\vec{r}-\vec{r}', h)$ = Kernel function

When discretised, Eq. (2) becomes Eq. (3) [15]. This represents the interpolation of all points within the support region of the Kernel function around the point of interest.

$$A(\vec{r}) = \sum_b m_b \frac{A_b}{\rho_b} W_{ab} \tag{3}$$

where

a = Interpolation point
A_b = Desired characteristic
ρ_b = Density of neighbouring particle
m_b = Mass of neighbouring particle
W_{ab} = Kernel function

2.1.1. Smoothing length

The smoothing length specifies the size of the influence domain that surrounds a certain particle. This determines the number of particles that the Kernel uses to interpolate particle properties. As a result, the smoothing length can have a large impact on the accuracy of the simulation, as it determines the quantity and quality of the particles used for interpolation. This is shown in Eq. (4) [5].

$$h = C_a\sqrt{dx^2 + dy^2 + dz^2} \tag{4}$$

where

h = Smoothing length
C_a = Smoothing length coefficient
$dx = dy = dz$ = Distance between particles

2.1.2. Courant–Friedrichs–Levy (CFL) condition

The CFL number is a parameter used to control the minimum time step required in order to ensure simulation stability. The CFL number combines both Courant and viscous time controls to ensure that each particle is exposed to the pressure wave propagating through the medium at each time step [5]. DualSPHysics requires this parameter to be entered between 0.2 and 0.5; however it is recommended to keep the value low to certify that the simulation captures the high energy fluid behaviour in a slamming event.

2.1.3. Artificial viscosity coefficient

The smoothed-particle method utilises an Eulerian approach to model the fluid flow within the simulation and therefore encounters similar problems to more conventional, mesh-based forms of Computational Fluid Dynamics (CFD) when it comes to approximating the viscosity term. Similar to mesh-based CFD, this viscosity term Θ, is therefore modelled to solve the continuum field.

$$\frac{D\vec{v}}{Dt} = -\frac{1}{\rho}\vec{\nabla}P + \vec{g} + \vec{\Theta} \tag{5}$$

Slamming problems have a relatively short duration and it was therefore decided that modelling the turbulence in the system to a high degree of accuracy would be more computationally demanding than the improvement in results would justify. As a result, the Artificial Viscosity model was chosen for use with the simulation, as it is the least computationally demanding of the three models provided by DualSPHysics.

$$\frac{d\vec{v}_a}{dt} = -\sum_b m_b\left(\frac{P_b}{{\rho^2}_b} - \frac{P_a}{{\rho^2}_a} + \prod_{ab}\right)\vec{\nabla}_a W_{ab} + \vec{g} \tag{6}$$

where

$g = (0, 0, -9.81) m/s^2$
$\prod_{ab}$ = Viscosity term

The viscosity term is defined by the following:

$$\prod_{ab} = \begin{cases} \dfrac{-\alpha\overline{c_{ab}}\mu_{ab}}{\rho_{ab}} & \vec{v}_{ab}\vec{r}_{ab} < 0 \\ 0 & \vec{v}_{ab}\vec{r}_{ab} > 0 \end{cases} \tag{7}$$

α is the artificial viscosity coefficient and alters the viscosity of the medium. It is altered for each simulation but is recommended as being taken to be 0.01 in most cases [16]. This will therefore be used as the basis for the numerical simulations; however it will also be investigated in an effort to determine the effect that it has on the simulation results.

2.2. SPH model

In order to quantify the effect of changing the input parameters on the results of the simulation, the numerical results were compared with data obtained from Whelan [21] who conducted an experiment with a freefalling wedge. As the geometry of the wedge used in the experiment has a uniform profile, it was decided that the SPH simulation would be conducted using the 2D projection of this wedge in order to decrease the computational power needed to obtain accurate results.

Fig. 3 shows the fluid domain and boundary conditions created in the SPH simulations. The wedge has a mass of 21.025 kg and a 3D depth (y-axis) of 290 mm. The tank is

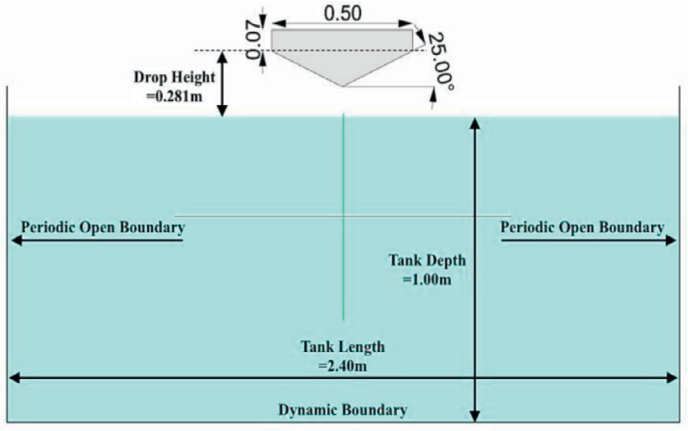

Fig. 3. Illustration of the initial simulation domain as is portrayed in Paraview (dimensions are in metres).

1 m deep and 2.4 m wide. The side (ZY) boundaries of the domain are periodic open boundaries and the bottom of the domain was defined as a dynamic boundary.

Releasing the wedge from the same drop height as the experimental test was considered to be an inefficient use of resources, as the program would have to calculate the properties of all the fluid particles at each time step whilst the wedge was falling. To improve this, the wedge was placed just above the free surface and given gravitational acceleration as well as an initial velocity, which was obtained from the experimental data as the velocity at the point of impact (1.705 m/s).

3. RANS VOF approach

3.1. RANS theory overview

The RANS simulations were conducted using commercial CFD solver STAR-CCM+ with an overset grid technique. The program resolves the incompressible RANS equation in integral form by utilising the finite volume technique. The free surface was modelled using the VOF method.

3.1.1. RANS equation and turbulence model

To solve the RANS equations, the instantaneous velocity and pressure fields are deconstructed into a mean value and a fluctuating component. Substituting these components into the non-dimensionalised continuity and momentum equations by using time averaging forms the basis for the RANS equation tensor derivation [3]:

$$\frac{\partial U_i}{\partial x_i} = 0 \tag{8}$$

$$\rho\left(\frac{\partial U_i}{\partial t}\right) + \rho\frac{\partial}{\partial x_j}(U_iU_j) = -\frac{\partial P}{\partial x_i} + \frac{\partial}{\partial x_j}(2\mu S_{ij} + \rho\tau_{ij}) \tag{9}$$

$$S_{ij} = \frac{1}{2}\left(\frac{\partial U_i}{\partial x_j} + \frac{\partial U_j}{\partial x_i}\right) \tag{10}$$

where

$U_{i(j)}$ = Time-averaged velocity

P = Pressure field

μ = Viscosity of the effective flow

ρ = Density of the effective flow

S_{ij} = Mean strain-rate tensor

$\tau_{ij} = \overline{-u_i'u_j'}$ = Reynold′s stress tensor

$u_{i(j)}'$ = Fluctuating velocity term in the timedomain

As the stress tensor remains unknown, additional equations are required to close the RANS equation and they are conventionally obtained from turbulence modelling. In the performed computations, closure of the Reynolds stress tensor is achieved by means of Menter's shear stress transport turbulence model. The transport behaviour of shear stress is achieved by constraining the value of kinematic eddy-viscosity. The approach adopts the K-Epsilon turbulence model in the far-field region and utilises the K-Omega model to solve flow near the wall.

3.1.2. Volume of Fluid (VOF)

The VOF method utilises the distribution of each phase at every time-step with reference to the given volume fraction [18]. Consequently the volume fraction for fluid i is defined as:

$$\alpha_i = \frac{V_i}{V} \tag{11}$$

For fluid i, the mass conversation can be considered in integral form:

$$\frac{\partial}{\partial t}\int_V \alpha_i dV + \int_S \alpha_i(\mathrm{v}\cdot\mathrm{n})dS = \int_V \left(s_{\alpha_i} - \frac{\alpha_i}{\rho_i}\frac{D\rho_i}{Dt}\right)dV \tag{12}$$

This is used by STAR-CCM+ to compute the volume fraction, α_i, transport properties. As a fraction, the sum of each component equation can be simplified using the following condition:

$$\sum_i \alpha_i = 1 \tag{13}$$

and

$$\rho = \sum_i \alpha_i\rho_i \tag{14}$$

By applying these simplifications to Eq. (12), the following integral form of the mass conservation law can be obtained as:

$$\int_S (\mathrm{v}\cdot\mathrm{n})dS = \sum_i \int_V \left(s_{\alpha_i} - \frac{\alpha_i}{\rho_i}\frac{D\rho_i}{Dt}\right)dV \quad (15)$$

3.1.3. Overset mesh

Utilizing an overset mesh within the discretization process allows mesh movement within the simulation. This method involves active cells utilizing regularly discretised equations, whereas an allocation of passive cells is temporarily or permanently deactivated (where no equation is solved). In the interface region there are active cells that refer to donor cells at another space within the grid. This acts as the link between the moving and static mesh [2]. The first layer of passive cells next to the active cells are called acceptor cells, where a minimum of 4 layers of complete cells between bodies and the overset boundaries are necessary for a reliant simulation. It is recommended that both cells in the overlapping zone are of comparable size (ideally 1:1 ratio) to maintain accuracy [2]. It is also necessary that the overset mesh cells do not move in the overlapping zone within one time step. As a result the minimum mesh size within the overset region and the time step used within the simulation are very important and should be carefully considered. However, regardless of efforts to reduce inaccuracies, a limitation within overset theory involves neglecting mass conservation at the interface. The error expected due to this limitation is in the order of less than 0.1% [2].

4. STAR-CCM+ model

4.1. Control volume and boundary conditions

The control volume of the fluid domain was constructed as shown in Fig. 4(a). To help define the physics settings, each face on the domain was named according to its respective boundary. Each of these faces was defined as a velocity inlet, symmetry side, overset boundary or wall. Within the background control volume, the following named selections were made:

Inlet/bottom/top/backwall: Each of these faces was set as velocity inlets. This boundary type meant that each face acts with a velocity acting in the pre-defined direction of the flat free surface. Both the inlet and backwall were set with volume fractions dependent on the flat wave characteristics, whereas the top was defined with purely air and the bottom with water.

Symside: The symmetry walls act as a simplification to the system in order to save computational resources. This boundary repeats the physics occurring on one side onto the reverse and causes an interaction accordingly.

Within the overset region, the following named selections were made:

Overset: This boundary defines the overset region, where the faces act as interfaces between the moving and static areas of the simulation.

Symside: The symmetry walls within the overset region are defined to be identical to those within the control volume.

Walls: The wall boundaries define where the impact of the water will occur. In the scenario of this simulation, the wall boundaries are the surface of the wedge itself.

4.2. Mesh

Fig. 4(b) is an illustration of the mesh constructed in STAR-CCM+. For the fluid domain and overset region, the mesh was defined separately by two different mesh continuums. Both continuums utilised surface remesher and trimmer cells to ensure that settings were customizable for convergence purposes. Within the fluid domain, volumetric controls were added for further refinement. These included:

Free surface refinement: A block part was created within the geometry to encompass the free surface. This prismatic layer was defined with customised anisotropic trimmer values in the x, y and z directions respectively.

Object path refinement: As the wedge is defined within an overset mesh and follows a path of movement, it was vital that the path was captured within the simulations with minimal errors. This geometry part was therefore created to ensure smooth transition with the path of motion.

5. Results and discussion

5.1. SPH parameter sensitivity study

The sensitivity studies into particle resolution, Kernel size and viscosity coefficient are detailed in the following. The particle resolution study was completed first, in order to obtain an optimal baseline to conduct the following simulations.

5.2. Particle resolution study

To assess the independency of the simulations from particle resolution, five different particle spacings were tested ranging from 0.016 m to 0.001 m. The accelerations of the object are displayed in Fig. 5 below. It can be observed that as the particle spacing is reduced, the instabilities in the simulation are lessened and tend towards experimental data from Whelan [21]. These instabilities are contributed to pressure waves propagating through the fluid, reflecting off the bottom of the simulation domain before impacting the falling wedge. This causes spikes in the acceleration profile, increasing the level of noise in the simulation. It can be stated that increasing the resolution of the domain reduces the severity of pressure waves in the medium, transforming them into smoother pressure variations rather than short duration impact forces. The 0.001 m particle resolution condition was therefore chosen for following parametric studies.

5.3. Smoothing Length Coefficient (SLC) study

The SLC was examined at values ranging from 0.85 to 1.35. These results were compared with experimental data

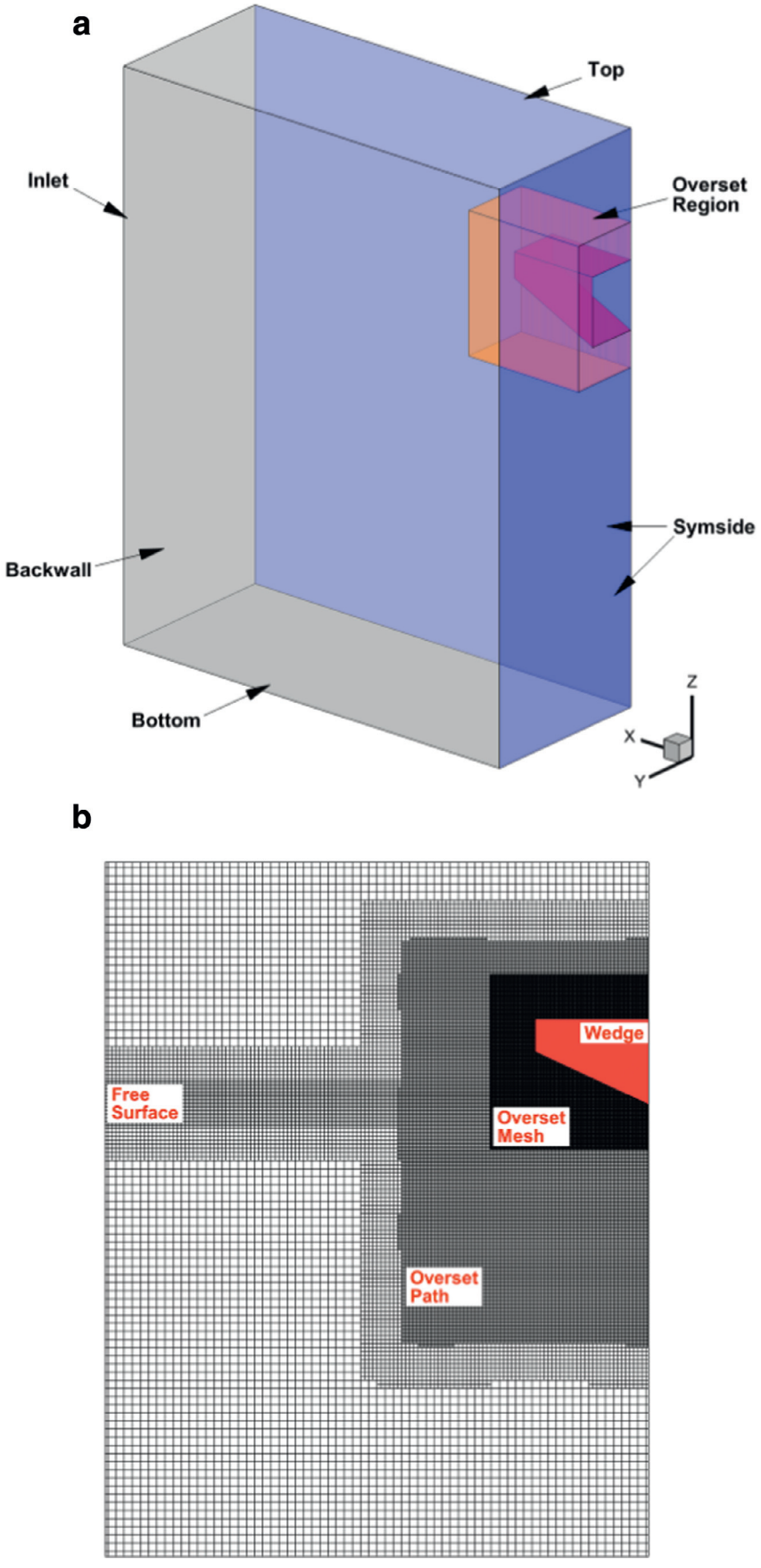

Fig. 4. Illustration of CFD modelling: (a) fluid domain; (b) mesh.

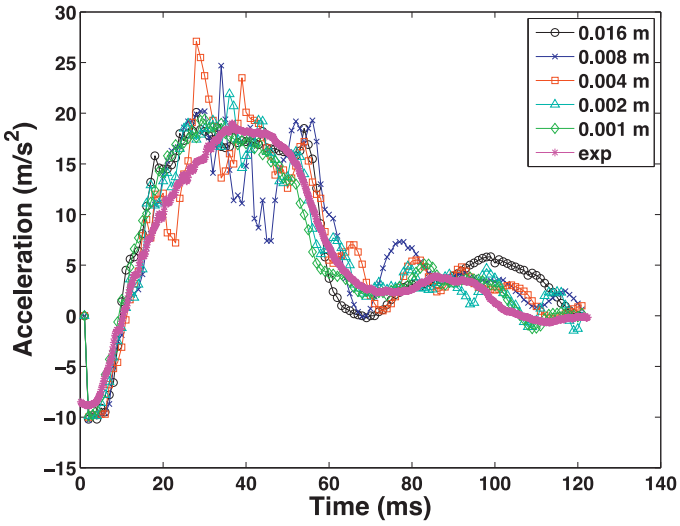

Fig. 5. The effect of changing the particle resolution on the accuracy of SPH acceleration results.

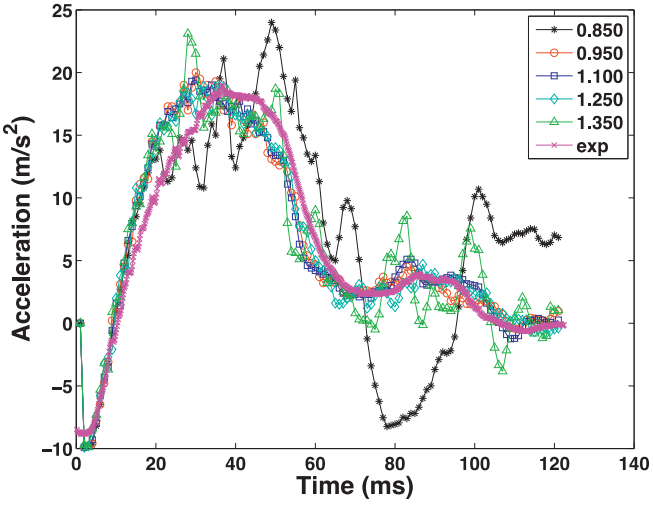

Fig. 6. The effect of varying the SLC on the acceleration of the free falling wedge in the SPH simulations.

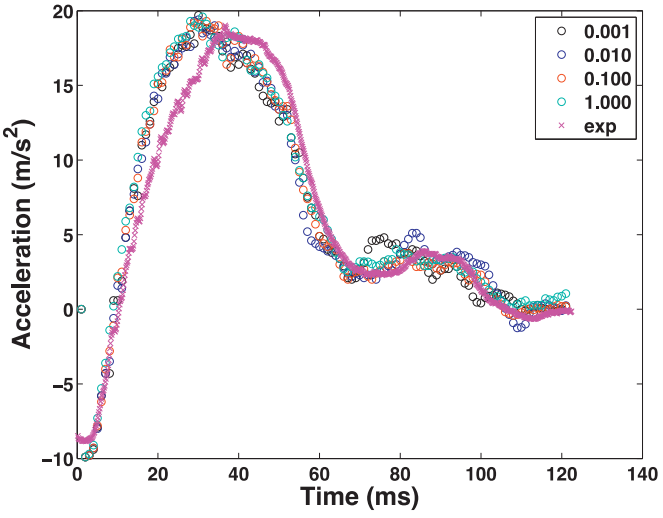

Fig. 7. The effect of varying the artificial viscosity on the acceleration of the free falling wedge.

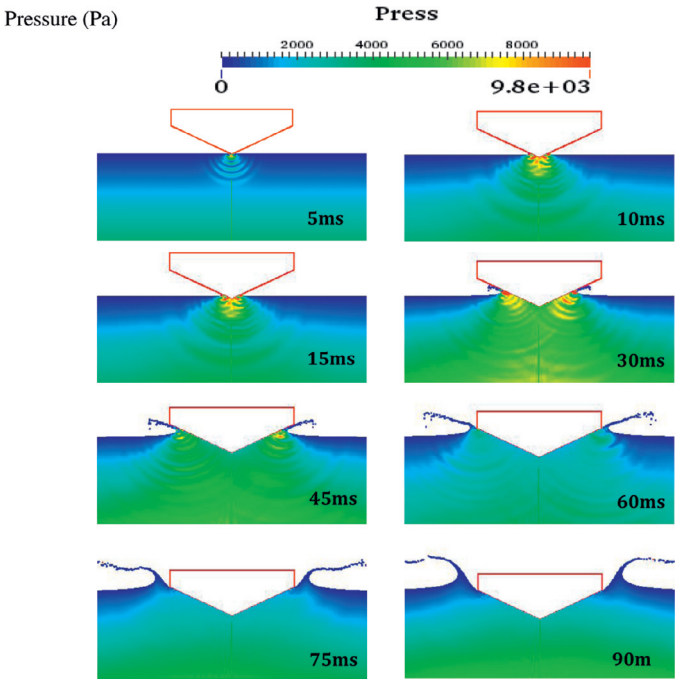

Fig. 8. Time captures of pressure distribution of the slamming impact from 5 to 90 ms displaying pressure variations in the fluid field.

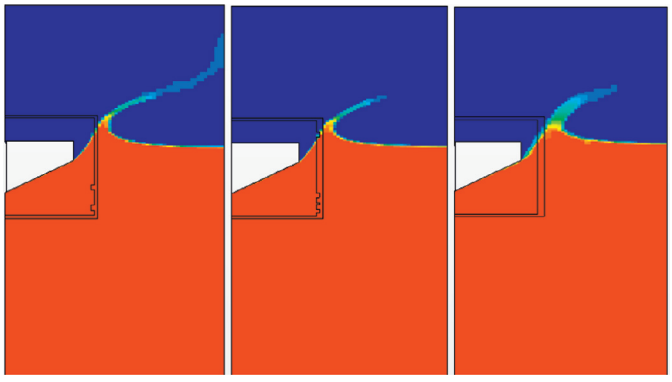

Fig. 9. Volume fraction plot at time step $t = 0.12$ s for CFL = 0.5 (left), CFL = 1 (middle) and CFL = 2 (right).

and are displayed in Fig. 6. The SLC analysis produced results that strongly suggest that the optimal Smoothing Length Coefficient is 1.1. It can be noticed in Fig. 6 that SLC values higher and lower than 1.1 are substantially more erratic. This is due to the number of particles that are used with the Kernel to interpolate the characteristic values of the fluid particles in the simulation. It is suggested that when the SLC is too large, particles are included in the interpolation, which, in reality, would not have any effect on the particle of interest. The opposite is true for small SLC values, which may provide too little information for the Kernel interpolation.

5.4. Viscosity coefficient analysis

Viscosity coefficients of 0.001, 0.01, 0.1 and 1 were simulated in SPH with the acceleration results being displayed in Fig. 7.

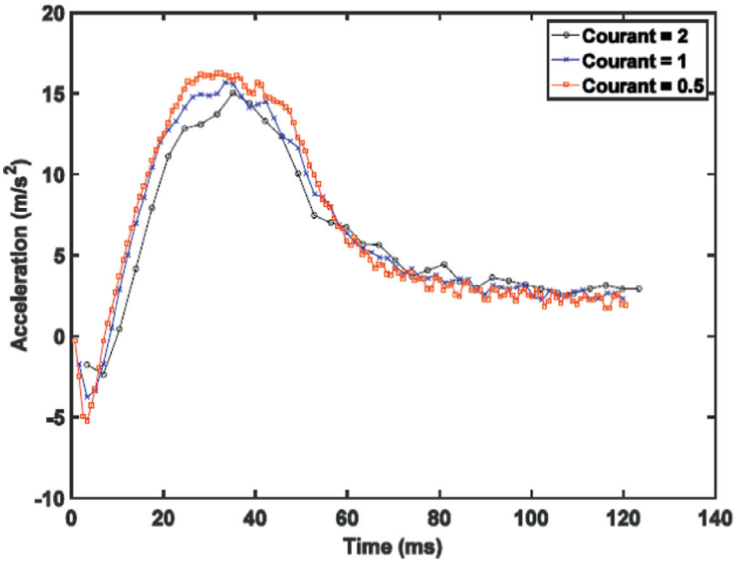

Fig. 10. Wedge drop acceleration profiles for various CFL number in the RANS computation.

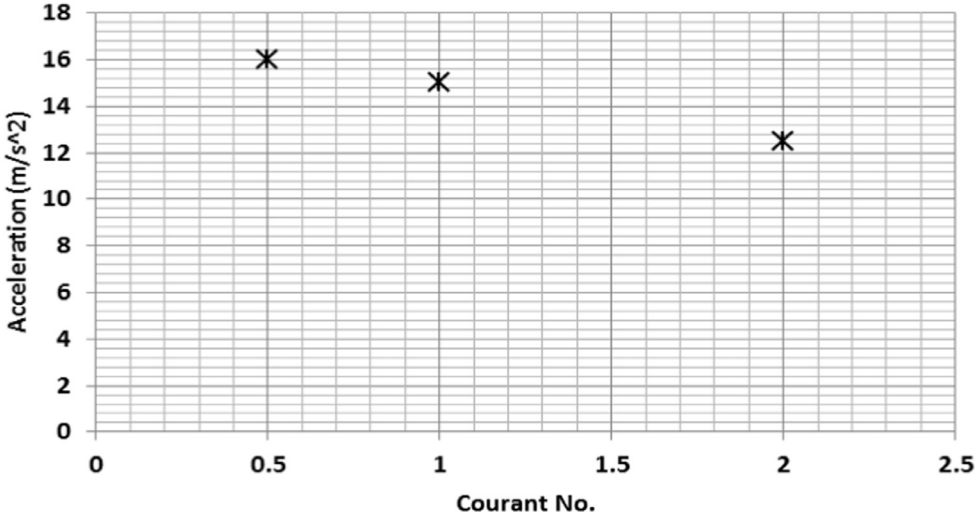

Fig. 11. Acceleration at time step $t = 25$ ms against CFL number in RANS computation.

As can be seen in Fig. 7, the alteration of the viscosity coefficient within a slamming investigation is not critical to the accuracy of the results. This is primarily because slamming impacts are short in duration and turbulence produced by a viscous medium is therefore not particularly important. This is because nearly the entire load on the impacting object is produced by the slamming impact, not viscous drag. When the wedge slows to a more constant sink rate, the difference between the results begins to rise. It is suggested that this behaviour is due to the increased affect viscous drag has on the movement of the object and therefore its acceleration profile.

5.5. Experimental vs. numerical results

Although studies of other parameters are not detailed in this paper, the results in SPH showed good correlation with the experimental data obtained from Whelan [21]. The data can be viewed in Fig. 5, where it can be observed that the error in the peak-slamming load at the finest resolution (0.001 m) amounts to less than 2% when compared to experimental data.

5.6. SPH results visualisation

Fig. 8 illustrates the pressure distribution of the particles and the formation of the fluid jet as the wedge impacts the water. The jet shows correct development, forming into a thin stream of particles at the edge of the impacting surface. It can also be noticed that the point of maximum pressure after initial impact is located where the jet is formed at the fluid surface.

6. RANS results

A time step sensitivity study for the RANS simulation is presented in this section. Three different time step values were adopted in the numerical model to investigate the impact of the CFL number on the simulation results.

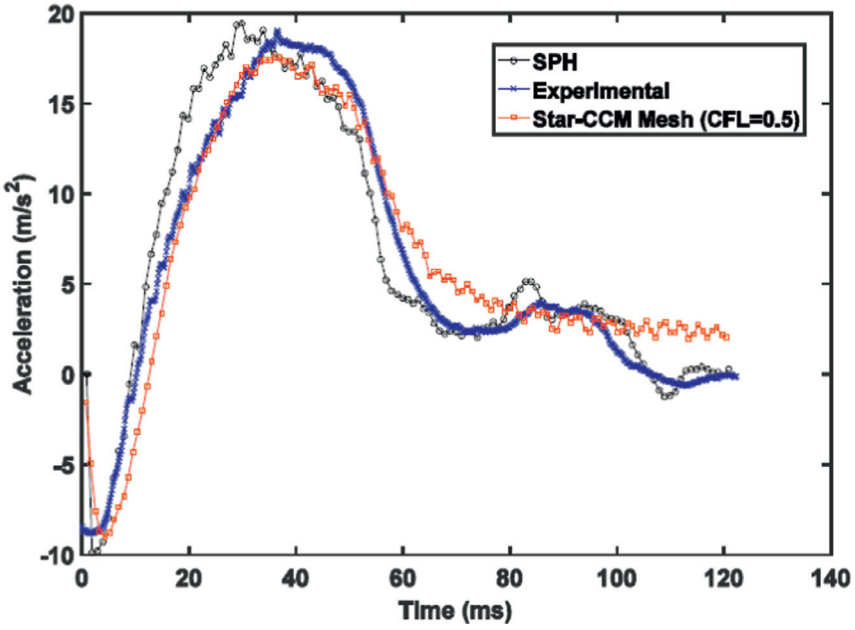

Fig. 12. Acceleration profile comparison between SPH, experimental and RANS results.

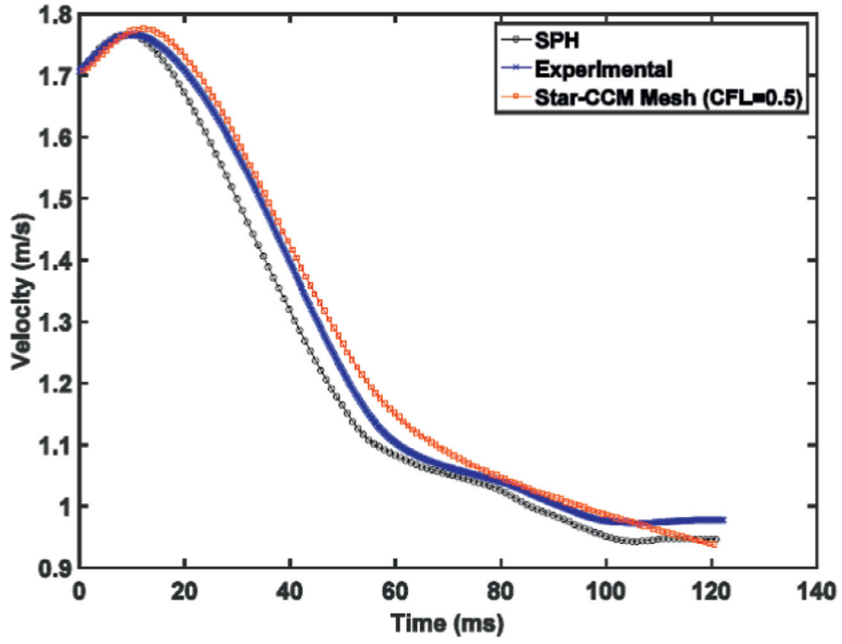

Fig. 13. Vertical velocity profile comparison between SPH, experimental and RANS results.

6.1. Effect of varying CFL number

As a consideration of the effect of changing the CFL number, the time step was altered with a ratio of two. Due to computational limitations, the mesh discretization remained constant throughout the simulations (it was found that coarsening the mesh caused instability within the simulations). A visual indication of the effect of changing the time step can be observed in Fig. 9. It can be noticed that although the mesh resolution remains the same for each case, the time step drastically changes the resolution of the splash caused by water entry. The effect can be seen in Fig. 9 and is quantified in Fig. 10.

It can be observed that the most significant difference in changing the time step is the magnitude of the buoyant acceleration experienced by the wedge. Since the acceleration profiles being compared are transient, it is hard to consider one instantaneous moment for convergence. However, it can be seen from the time history that from 20 ms to 30 ms the buoyancy force is at a maximum for each CFL case. Another example of this steady condition can be noticed in the rise to peak buoyancy force (time history 10-20 ms). The relative

discrepancies between each CFL case at the peak buoyancy force are plotted in Fig. 11.

6.2. SPH results vs CFD predictions

From the consideration of pre-existing experimental data, the simple geometry considered was simulated for 0.12 s in both the SPH and RANS computations. The purpose of this investigation is to prove credibility of these two methodologies by comparing them to experimental results.

In the RANS simulation, it was found that a CFL value of 0.5 was necessary to obtain valid results. This has been adopted in this study, with the subsequent acceleration profile being compared with the SPH results and experimental data in Fig. 12 below.

From Fig. 12, it can be seen that both the SPH and RANS results follow the general profile of the experimental data; where the acceleration profiles peak at around 40 ms, with an acceleration of 17.5 ms^{-2}. It can be observed that the water entry and peak accelerations in the RANS model occur approximately 2 ms after the experimental. Whereas for the SPH simulation, the acceleration reaches its maximum at 5 ms ahead of the experimental data. From 60 ms onwards it can be seen that RANS appears to average out the oscillatory movement, resulting in higher frequency oscillations.

As a further consideration, Fig. 13 shows the velocity profile for each respective case. It can be observed that the residual difference between the experimental and RANS results prior to 50 ms is much smaller than that of the experimental and SPH results. The large frequency oscillations from 60 ms onwards within the simulation are averaged in RANS however, which may explain the small difference in results. This may need to be further monitored in future simulations.

7. Conclusions

After conducting a series of sensitivity analyses on the freefalling wedge it can be confidently stated that both SPH and RANS are highly accurate methods of predicting the slamming loads on simple falling geometries. The following conclusions can be drawn:

- The particle resolution in SPH has a great impact on the accuracy and stability of the slamming load estimation by reducing the impact of pressure waves on the motion of the impacting body.
- The Smoothing Length Coefficient in SPH also plays an important role in slamming load estimation and should be carefully determined by sensitivity analysis. The optimal value used for this analysis was determined to be 1.1. The viscosity coefficient has the smallest impact on slamming load estimation, with the value of 0.01 recommended by Monaghan [16] producing accurate results. It is advised that this value be used for future simulations.
- The CFL number in RANS has a pronounced influence on the computed acceleration profile and slamming loads. By varying the discretisation time step, the simulation achieved different levels of accuracy. Simulations with a small CFL number were found to produce more reliable predictions.
- Comparing the numerical results with experimental data, it was found that both methods are capable of modelling harsh slamming impacts. The RANS method slightly better predicts the acceleration values prior to peak acceleration, while the quick setup of SPH simulations, together with the use of GPU accelerated computing, gives advantages to the SPH method.

References

[1] A.C. Crespo, J.M. Dominguez, A. Barreiro, M. Gómez-Gesteira, B.D. Rogers, PloS one 6 (6) (2011) e20685.
[2] CD-Adapco, in: Paper presented at the STAR South East Asian Conference, Kuala Lumper, 2013.
[3] CD-Adapco. (2014). User guide STARCCM+ Version 9.0.6.
[4] J.M. Domínguez, A.J. Crespo, M. Gómez-Gesteira, Comput. Phys. Commun. 184 (3) (2013) 617–627.
[5] Gesteira, M.G., Rogers, B.D., Dalrymple, R.A., Crespo, A.J.C., & Narayanaswamy, M. (2010). A user guide for the SPHysics code.
[6] R.A. Gingold, J.J. Monaghan, Smoothed Particle Hydrodynamics: Theory and Application to Non-Spherical Stars, Cambridge: Institute of Astronomy, 1977.
[7] M. Gomez-Gesteira, A.J. Crespo, B.D. Rogers, R. Dalrymple, J.M. Dominguez, A. Barreiro, Comput. Geosci. 48 (2012) 300–307.
[8] M. Gomez-Gesteira, B.D. Rogers, A.J. Crespo, R. Dalrymple, M. Narayanaswamy, J.M. Dominguez, Comput. Geosci. 48 (2012) 289–299.
[9] M. Gomez-Gesteira, B.D. Rogers, R.A. Dalrymple, A.J. Crespo, J. Hydraul. Res. 48 (S1) (2010) 6–27.
[10] J.R. Henry, F.C. Bailey, Slamming of Ships: A Critical Review of the Current State of Knowledge, U.S. Coast Guard, Washington D.C, USA, 1970.
[11] S.R. Johannessen, Use of CFD to Study Hydrodynamic Loads on Free–Fall Lifeboats in the Impact Phase. (Master of Science), NTNU, Trondheim, 2012.
[12] G.K. Kapsenburg, Philosop. Trans. R. Soc. A 369 (2011) 2892–2919.
[13] E. Larsen, Impact Loads on Circular Cylinders. (Master of Science), Norwegian University of Science and Technology, Trondheim, 2013.
[14] G.R. Liu, M.B. Liu, Smoothed Particle Hydrodynamics: a Meshfree Particle Method, 1, World Scientific Publishing Company, Singapore, 2003.
[15] J.J. Monaghan, Annu. Rev. Astronom. Astrophys. 30 (1992) 543–574.
[16] J.J. Monaghan, J. Comput. Phys. 110 (2) (1994) 399–406.
[17] G. Oger, M. Doring, B. Alessandrini, P. Ferrant, J. Comput. Phys. 213 (2005) 803–822.
[18] CD-ADAPCO, User guide STAR-CCM+ Version 9.0.6., 2014.
[19] M. Tak, D. Park, T. Park, J. Eng. Mater. Technol. 135 (2) (2013) 021013.
[20] H. Wagner, Z. Angew. Math. Mech. (12) (1932) 193–215.
[21] J.R. Whelan, (2004). Wetdeck slamming of high-speed catamarans with a centre bow/by James R. Whelan: 2004.